EUROPEAN ORGANISATION FOR NUCLEAR RESEARCH

CERN-EP/99-169
29 November 1999

Search for Unstable Heavy and Excited Leptons at LEP2

The OPAL Collaboration

Abstract

Searches for unstable neutral and charged heavy leptons, N and $L^{\pm}$, and for excited states of neutral and charged leptons, ν^*, e^*, μ^*, and τ^*, have been performed in e^+e^- collisions using data collected by the OPAL detector at LEP. The data analysed correspond to an integrated luminosity of about 58 pb^{-1} at a centre-of-mass energy of 183 GeV, and about 10 pb^{-1} each at 161 GeV and 172 GeV. No evidence for new particles was found. Lower limits on the masses of unstable heavy and excited leptons are derived. From the analysis of charged-current, neutral-current, and photonic decays of singly produced excited leptons, upper limits are determined for the ratio of the coupling to the compositeness scale, f/Λ, for masses up to the kinematic limit. For excited leptons, the limits are established independently of the relative values of the coupling constants f and f'.

(submitted to Eur. Phys. J. C)

G. Abbiendi[2], K. Ackerstaff[8], P.F. Akesson[3], G. Alexander[23], J. Allison[16], K.J. Anderson[9], S. Arcelli[17], S. Asai[24], S.F. Ashby[1], D. Axen[29], G. Azuelos[18,a], I. Bailey[28], A.H. Ball[8], E. Barberio[8], R.J. Barlow[16], J.R. Batley[5], S. Baumann[3], T. Behnke[27], K.W. Bell[20], G. Bella[23], A. Bellerive[9], S. Bentvelsen[8], S. Bethke[14,i], S. Betts[15], O. Biebel[14,i], A. Biguzzi[5], I.J. Bloodworth[1], P. Bock[11], J. Böhme[14,h], O. Boeriu[10], D. Bonacorsi[2], M. Boutemeur[33], S. Braibant[8], P. Bright-Thomas[1], L. Brigliadori[2], R.M. Brown[20], H.J. Burckhart[8], P. Capiluppi[2], R.K. Carnegie[6], A.A. Carter[13], J.R. Carter[5], C.Y. Chang[17], D.G. Charlton[1,b], D. Chrisman[4], C. Ciocca[2], P.E.L. Clarke[15], E. Clay[15], I. Cohen[23], J.E. Conboy[15], O.C. Cooke[8], J. Couchman[15], C. Couyoumtzelis[13], R.L. Coxe[9], M. Cuffiani[2], S. Dado[22], G.M. Dallavalle[2], S. Dallison[16], R. Davis[30], A. de Roeck[8], P. Dervan[15], K. Desch[27], B. Dienes[32,h], M.S. Dixit[7], M. Donkers[6], J. Dubbert[33], E. Duchovni[26], G. Duckeck[33], I.P. Duerdoth[16], P.G. Estabrooks[6], E. Etzion[23], F. Fabbri[2], A. Fanfani[2], M. Fanti[2], A.A. Faust[30], L. Feld[10], P. Ferrari[12], F. Fiedler[27], M. Fierro[2], I. Fleck[10], A. Frey[8], A. Fürtjes[8], D.I. Futyan[16], P. Gagnon[12], J.W. Gary[4], G. Gaycken[27], C. Geich-Gimbel[3], G. Giacomelli[2], P. Giacomelli[2], D.M. Gingrich[30,a], D. Glenzinski[9], J. Goldberg[22], W. Gorn[4], C. Grandi[2], K. Graham[28], E. Gross[26], J. Grunhaus[23], M. Gruwé[27], C. Hajdu[31] G.G. Hanson[12], M. Hansroul[8], M. Hapke[13], K. Harder[27], A. Harel[22], C.K. Hargrove[7], M. Harin-Dirac[4], M. Hauschild[8], C.M. Hawkes[1], R. Hawkings[27], R.J. Hemingway[6], G. Herten[10], R.D. Heuer[27], M.D. Hildreth[8], J.C. Hill[5], P.R. Hobson[25], A. Hocker[9], K. Hoffman[8], R.J. Homer[1], A.K. Honma[8], D. Horváth[31,c], K.R. Hossain[30], R. Howard[29], P. Hüntemeyer[27], P. Igo-Kemenes[11], D.C. Imrie[25], K. Ishii[24], F.R. Jacob[20], A. Jawahery[17], H. Jeremie[18], M. Jimack[1], C.R. Jones[5], P. Jovanovic[1], T.R. Junk[6], N. Kanaya[24], J. Kanzaki[24], G. Karapetian[18], D. Karlen[6], V. Kartvelishvili[16], K. Kawagoe[24], T. Kawamoto[24], P.I. Kayal[30], R.K. Keeler[28], R.G. Kellogg[17], B.W. Kennedy[20], D.H. Kim[19], A. Klier[26], T. Kobayashi[24], M. Kobel[3], T.P. Kokott[3], M. Kolrep[10], S. Komamiya[24], R.V. Kowalewski[28], T. Kress[4], P. Krieger[6], J. von Krogh[11], T. Kuhl[3], M. Kupper[26], P. Kyberd[13], G.D. Lafferty[16], H. Landsman[22], D. Lanske[14], J. Lauber[15], I. Lawson[28], J.G. Layter[4], D. Lellouch[26], J. Letts[12], L. Levinson[26], R. Liebisch[11], J. Lillich[10], B. List[8], C. Littlewood[5], A.W. Lloyd[1], S.L. Lloyd[13], F.K. Loebinger[16], G.D. Long[28], M.J. Losty[7], J. Lu[29], J. Ludwig[10], A. Macchiolo[18], A. Macpherson[30], W. Mader[3], M. Mannelli[8], S. Marcellini[2], T.E. Marchant[16], A.J. Martin[13], J.P. Martin[18], G. Martinez[17], T. Mashimo[24], P. Mättig[26], W.J. McDonald[30], J. McKenna[29], E.A. Mckigney[15], T.J. McMahon[1], R.A. McPherson[28], F. Meijers[8], P. Mendez-Lorenzo[33], F.S. Merritt[9], H. Mes[7], I. Meyer[5], A. Michelini[2], S. Mihara[24], G. Mikenberg[26], D.J. Miller[15], W. Mohr[10], A. Montanari[2], T. Mori[24], K. Nagai[8], I. Nakamura[24], H.A. Neal[12,f], R. Nisius[8], S.W. O'Neale[1], F.G. Oakham[7], F. Odorici[2], H.O. Ogren[12], A. Okpara[11], M.J. Oreglia[9], S. Orito[24], G. Pásztor[31], J.R. Pater[16], G.N. Patrick[20], J. Patt[10], R. Perez-Ochoa[8], S. Petzold[27], P. Pfeifenschneider[14], J.E. Pilcher[9], J. Pinfold[30], D.E. Plane[8], B. Poli[2], J. Polok[8], M. Przybycień[8,d], A. Quadt[8], C. Rembser[8], H. Rick[8], S.A. Robins[22], N. Rodning[30], J.M. Roney[28], S. Rosati[3], K. Roscoe[16], A.M. Rossi[2], Y. Rozen[22], K. Runge[10], O. Runolfsson[8], D.R. Rust[12], K. Sachs[10], T. Saeki[24], O. Sahr[33], W.M. Sang[25], E.K.G. Sarkisyan[23], C. Sbarra[28], A.D. Schaile[33], O. Schaile[33], P. Scharff-Hansen[8], J. Schieck[11], S. Schmitt[11], A. Schöning[8], M. Schröder[8], M. Schumacher[3], C. Schwick[8], W.G. Scott[20], R. Seuster[14,h], T.G. Shears[8], B.C. Shen[4], C.H. Shepherd-Themistocleous[5], P. Sherwood[15], G.P. Siroli[2], A. Skuja[17], A.M. Smith[8], G.A. Snow[17], R. Sobie[28], S. Söldner-Rembold[10,e], S. Spagnolo[20], M. Sproston[20], A. Stahl[3], K. Stephens[16], K. Stoll[10], D. Strom[19], R. Ströhmer[33], B. Surrow[8], R. Tafirout[18,j], S.D. Talbot[1], P. Taras[18], S. Tarem[22], R. Teuscher[9], M. Thiergen[10], J. Thomas[15], M.A. Thomson[8], E. Torrence[8], S. Towers[6], T. Trefzger[33], I. Trigger[18], Z. Trócsányi[32,g], E. Tsur[23], M.F. Turner-Watson[1], I. Ueda[24], R. Van Kooten[12], P. Vannerem[10], M. Verzocchi[8],

H. Voss[3], F. Wäckerle[10], D. Waller[6], C.P. Ward[5], D.R. Ward[5], P.M. Watkins[1], A.T. Watson[1], N.K. Watson[1], P.S. Wells[8], T. Wengler[8], N. Wermes[3], D. Wetterling[11] J.S. White[6], G.W. Wilson[16], J.A. Wilson[1], T.R. Wyatt[16], S. Yamashita[24], V. Zacek[18], D. Zer-Zion[8]

[1]School of Physics and Astronomy, University of Birmingham, Birmingham B15 2TT, UK
[2]Dipartimento di Fisica dell' Università di Bologna and INFN, I-40126 Bologna, Italy
[3]Physikalisches Institut, Universität Bonn, D-53115 Bonn, Germany
[4]Department of Physics, University of California, Riverside CA 92521, USA
[5]Cavendish Laboratory, Cambridge CB3 0HE, UK
[6]Ottawa-Carleton Institute for Physics, Department of Physics, Carleton University, Ottawa, Ontario K1S 5B6, Canada
[7]Centre for Research in Particle Physics, Carleton University, Ottawa, Ontario K1S 5B6, Canada
[8]CERN, European Organisation for Particle Physics, CH-1211 Geneva 23, Switzerland
[9]Enrico Fermi Institute and Department of Physics, University of Chicago, Chicago IL 60637, USA
[10]Fakultät für Physik, Albert Ludwigs Universität, D-79104 Freiburg, Germany
[11]Physikalisches Institut, Universität Heidelberg, D-69120 Heidelberg, Germany
[12]Indiana University, Department of Physics, Swain Hall West 117, Bloomington IN 47405, USA
[13]Queen Mary and Westfield College, University of London, London E1 4NS, UK
[14]Technische Hochschule Aachen, III Physikalisches Institut, Sommerfeldstrasse 26-28, D-52056 Aachen, Germany
[15]University College London, London WC1E 6BT, UK
[16]Department of Physics, Schuster Laboratory, The University, Manchester M13 9PL, UK
[17]Department of Physics, University of Maryland, College Park, MD 20742, USA
[18]Laboratoire de Physique Nucléaire, Université de Montréal, Montréal, Quebec H3C 3J7, Canada
[19]University of Oregon, Department of Physics, Eugene OR 97403, USA
[20]CLRC Rutherford Appleton Laboratory, Chilton, Didcot, Oxfordshire OX11 0QX, UK
[22]Department of Physics, Technion-Israel Institute of Technology, Haifa 32000, Israel
[23]Department of Physics and Astronomy, Tel Aviv University, Tel Aviv 69978, Israel
[24]International Centre for Elementary Particle Physics and Department of Physics, University of Tokyo, Tokyo 113-0033, and Kobe University, Kobe 657-8501, Japan
[25]Institute of Physical and Environmental Sciences, Brunel University, Uxbridge, Middlesex UB8 3PH, UK
[26]Particle Physics Department, Weizmann Institute of Science, Rehovot 76100, Israel
[27]Universität Hamburg/DESY, II Institut für Experimental Physik, Notkestrasse 85, D-22607 Hamburg, Germany
[28]University of Victoria, Department of Physics, P O Box 3055, Victoria BC V8W 3P6, Canada
[29]University of British Columbia, Department of Physics, Vancouver BC V6T 1Z1, Canada
[30]University of Alberta, Department of Physics, Edmonton AB T6G 2J1, Canada
[31]Research Institute for Particle and Nuclear Physics, H-1525 Budapest, P O Box 49, Hungary
[32]Institute of Nuclear Research, H-4001 Debrecen, P O Box 51, Hungary
[33]Ludwigs-Maximilians-Universität München, Sektion Physik, Am Coulombwall 1, D-85748 Garching, Germany

[a] and at TRIUMF, Vancouver, Canada V6T 2A3
[b] and Royal Society University Research Fellow
[c] and Institute of Nuclear Research, Debrecen, Hungary
[d] and University of Mining and Metallurgy, Cracow
[e] and Heisenberg Fellow
[f] now at Yale University, Dept of Physics, New Haven, USA
[g] and Department of Experimental Physics, Lajos Kossuth University, Debrecen, Hungary
[h] and MPI München
[i] now at MPI für Physik, 80805 München
[j] now at Laurentian University, Physics & Astronomy, Sudbury, Canada, P3E 2C6.

1 Introduction

In spite of its remarkable success in describing all electroweak data available today, the Standard Model (SM) [1] leaves many questions unanswered. In particular, it explains neither the origin of the number of fermion generations nor the fermion mass spectrum. The precise measurements of the electroweak parameters at the Z pole have shown that the number of species of light neutrinos is three [2]; however, this does not exclude a fourth generation, or other massive fermions, if these particles have masses greater than half the mass of the Z-boson ($M_{\mathrm{Z}}/2$).

New fermions could be of the following types (for reviews see References [3–5]): sequential fermions, mirror fermions (with chirality opposite to that in the SM), vector fermions (with left- and right-handed doublets), and singlet fermions. These could be produced at high-energy $\mathrm{e^+e^-}$ colliders such as LEP, where two production mechanisms are possible: pair-production and single-production in association with a light standard fermion.

Lower limits on the masses of heavy leptons were obtained in $\mathrm{e^+e^-}$ collisions at centre-of-mass energies, $\sqrt{s}$, around M_{Z} [2, 6], and recent searches at $\sqrt{s}$ = 130-140 GeV [7, 8], $\sqrt{s}$ = 161 GeV [9, 10], $\sqrt{s}$ = 172 GeV [10, 11] and $\sqrt{s}$ = 130-183 GeV [12, 13] have improved these limits. Excited leptons have been sought at $\sqrt{s} \sim M_{\mathrm{Z}}$ [14], $\sqrt{s}$ = 130-140 GeV [15, 16], $\sqrt{s}$ = 161 GeV [17, 18], $\sqrt{s}$ = 172 GeV [11], $\sqrt{s}$ = 183 GeV [13], $\sqrt{s}$ = 189 GeV [19], and at the HERA ep collider [20]. If direct production is kinematically forbidden, the cross-sections of processes such as $\mathrm{e^+e^-} \to \gamma\gamma$ and $\mathrm{e^+e^-} \to \mathrm{f\bar{f}}$ [21, 22] are sensitive to new particles at higher masses.

This paper concentrates on the search conducted by OPAL [23] in a wide range of topologies for the pair-production of new unstable heavy leptons and for both pair- and single-production of excited leptons of the known generations, using data collected in 1997 at $\sqrt{s} = 181-184$ GeV, with an average energy of 182.7 GeV. The integrated luminosity used depends on the final-state topologies, and is between 52 and 58 $\mathrm{pb^{-1}}$. The results are combined with those obtained earlier from 10 $\mathrm{pb^{-1}}$ of data at $\sqrt{s} = 161.3$ GeV and 10 $\mathrm{pb^{-1}}$ at $\sqrt{s} = 172.1$ GeV.

1.1 Heavy Leptons

Heavy neutral leptons are particularly interesting in the light of recent evidence for massive SM neutrinos [24, 25]. One method of generating neutrino mass is the see-saw mechanism [26], which predicts additional heavy neutral leptons. In this mechanism, if the mass of a heavy neutral lepton satisfies the relation $m_{\mathrm{N}} = m_{\mathrm{e}}^2/m_{\nu_{\mathrm{e}}}$, and if $m_{\nu_{\mathrm{e}}}$ is as massive as 2.5 eV, then $m_{\mathrm{N}} \approx 100$ GeV, which is within the reach of LEP2.

In general, new heavy leptons N and $\mathrm{L^\pm}$ could in principle decay through the charged (CC) or neutral current (NC) channels:

$$\mathrm{N} \to \ell^\pm \mathrm{W}^\mp \quad , \quad \mathrm{N} \to \mathrm{L}^\pm \mathrm{W}^\mp \quad , \quad \mathrm{N} \to \nu_\ell \mathrm{Z},$$

$$\mathrm{L}^\pm \to \nu_\ell \mathrm{W}^\pm \quad , \quad \mathrm{L}^\pm \to \mathrm{N_L W}^\pm \quad , \quad \mathrm{L}^\pm \to \ell^\pm \mathrm{Z},$$

where $\mathrm{N_L}$ is a stable or long-lived neutral heavy lepton, and $\ell = \mathrm{e},\ \mu,$ or τ. For heavy lepton masses less than the gauge boson masses, M_{W} or M_{Z}, the vector bosons are virtual, leading to 3-body decay topologies. For masses greater than M_{W} or M_{Z}, the decays are 2-body decays, and the CC and NC branching ratios can be comparable. For masses close to M_{W} or M_{Z}, it is important to treat the transition from the 3-body to the 2-body decay properly, including effects from the vector boson widths. Expressions for the computation of partial decay widths with an off-shell W or Z boson can be found in [4].

The mixing of a heavy lepton with the standard lepton flavour is governed by a mixing angle ζ. A mixing of 0.01 radians yields a decay length $c\tau$ of $\mathcal{O}(1$ nm). Since the decay length is proportional to $1/\zeta^2$, looking for unstable heavy leptons which decay within the first cm, the analyses described in this paper are sensitive to $\zeta^2 > \mathcal{O}(10^{-12})$. The presently existing upper limit on ζ^2 is approximately 0.005 radians^2 [27].

The searches for heavy leptons presented in this paper utilise only the case where N and $\mathrm{L}^{\pm}$ decay via the CC channel, as would be expected in a naive fourth generation extension to the SM. The NC channel does not contribute significantly in the heavy lepton searches due to kinematics. Searches for stable or long-lived charged heavy leptons, $\mathrm{L}^{\pm}$, are described in a separate paper [12].

1.2 Excited Leptons

Compositeness models [5] attempt to explain the hierarchy of masses in the SM by the existence of a substructure within the fermions. Several of these models predict excited states of the known leptons. Excited leptons are assumed to have the same electroweak SU(2) and U(1) gauge couplings, g and g', to the vector bosons, but are expected to be grouped into both left- and right-handed weak isodoublets with vector couplings. The existence of the right-handed doublets is required to protect the ordinary light leptons from radiatively acquiring a large anomalous magnetic moment via the $\ell^*\ell V$ interaction [5] (where V is a γ, Z, or $\mathrm{W}^{\pm}$ and ℓ^* refers in this case to both charged and neutral excited leptons).

In $\mathrm{e^+e^-}$ collisions, excited leptons could be produced in pairs via the process $\mathrm{e^+e^-} \to \ell^*\bar{\ell}^*$, or singly via the process $\mathrm{e^+e^-} \to \ell^*\bar{\ell}$, as a result of the $\ell^*\ell V$ couplings. Depending on the details of these couplings, excited leptons could be detected in the photonic, CC, or NC channels:

$$\nu_\ell^* \to \nu_\ell\gamma \quad , \quad \nu_\ell^* \to \ell^{\pm}\mathrm{W}^{\mp} \quad , \quad \nu_\ell^* \to \nu_\ell\mathrm{Z},$$

$$\ell^{*\pm} \to \ell^{\pm}\gamma \quad , \quad \ell^{*\pm} \to \nu_\ell\mathrm{W}^{\pm} \quad , \quad \ell^{*\pm} \to \ell^{\pm}\mathrm{Z},$$

where ν_ℓ^* and $\ell^{*\pm}$ are neutral and charged excited leptons, respectively.

The branching fractions of the excited leptons into the different vector bosons are determined by the strength of the three $\ell^*\ell V$ couplings. We use the effective Lagrangian [5]:

$$\mathcal{L}_{\ell\ell^*} = \frac{1}{2\Lambda}\bar{\ell}^*\sigma^{\mu\nu}\left[gf\frac{\boldsymbol{\tau}}{2}\mathbf{W}_{\mu\nu} + g'f'\frac{Y}{2}B_{\mu\nu}\right]\ell_{\mathrm{L}} + \text{hermitian conjugate}, \qquad (1)$$

which describes the generalized magnetic de-excitation of the excited states. The matrix $\sigma^{\mu\nu}$ is the covariant bilinear tensor, $\boldsymbol{\tau}$ are the Pauli matrices, $\mathbf{W}_{\mu\nu}$ and $B_{\mu\nu}$ represent the fully gauge-invariant field tensors, and Y is the weak hypercharge. The parameter Λ has units of energy and can be regarded as the compositeness scale, while f and f' are the weights associated with the different gauge groups.

The relative values of f and f' also affect the size of the single-production cross-sections and their detection efficiencies. Depending on their relative values, either the photonic decay, the CC decay, or the NC decay will have the largest branching fraction, depending on the respective couplings [5]:

$$f_\gamma = e_f f' + I_{3L}(f - f') \quad , \quad f_W = \frac{f}{\sqrt{2}s_w} \quad , \quad f_Z = \frac{4I_{3L}(c_w^2 f + s_w^2 f') - 4e_f s_w^2 f'}{4 s_w c_w}$$

where e_f is the excited fermion charge, I_{3L} is the weak isospin, and $s_w(c_w)$ are the sine (cosine) of the Weinberg angle θ_w.

Our results will be interpreted using the two complementary coupling assignments, $f = f'$ and $f = -f'$. For example, for the case $f = -f'$, the photonic coupling to excited electrons is suppressed and the dominant production of excited electrons is via the s-channel. For $f \neq -f'$, the t-channel production of excited electrons dominates. In the case of excited neutrinos, if $f \neq f'$, then the photonic coupling is allowed. In addition to the results for the two assignments $f = f'$ and $f = -f'$, a new method is introduced which gives limits on excited leptons independent of the relative values of f and f'.

2 Monte Carlo Simulation

The Monte Carlo (MC) generator EXOTIC [28] has been used for the simulation of heavy lepton pair-production, $e^+e^- \to N\bar{N}$ and $e^+e^- \to L^+L^-$, of excited lepton pair-production, $e^+e^- \to \nu_\ell^* \bar{\nu}_\ell^*$ and $e^+e^- \to \ell^{*+}\ell^{*-}$, and of single excited lepton production, $e^+e^- \to \nu_\ell^* \bar{\nu}_\ell$ and $e^+e^- \to \ell^* \ell$. The code is based on formulae given in [4, 29]. The matrix elements include all spin correlations in the production and decay processes, and describe the transition from 3-body to 2-body decays of heavy fermions, involving virtual or real vector bosons, including the effects from vector boson widths. The JETSET [30] package is used for the fragmentation and hadronization of quarks.

For $N\bar{N}$ and L^+L^- production, MC samples were generated for a set of masses from 40 to 90 GeV. Separate samples were generated for Dirac and Majorana heavy neutral leptons, taking into account the different angular distributions. For the case where $L^- \to N_L W^-$, samples were simulated at 25 points in the (M_L,M_{N_L}) plane with M_L ranging from 50 to 90 GeV and M_{N_L} from 40 to 87 GeV, and with a mass difference $M_L - M_{N_L}$ larger than 3 GeV. Excited lepton MC samples were generated for the pair-production channels with masses in the range from 40 to 90 GeV and for the single-production channels with masses in the range from 90 to 180 GeV.

A variety of MC generators was used to study the multihadronic background from SM processes: 4-fermion background processes were simulated using the generator grc4f [31], multihadronic background from 2-fermion final states was modelled using PYTHIA [30], while

2-photon processes were generated with PHOJET [32] and HERWIG [33]. To study the background from low-multiplicity events, the generators BHWIDE [34] (large-angle Bhabha scattering) and TEEGG [35] (t-channel Bhabha scattering) were used for the $e^+e^-\gamma(\gamma)$ topology. The KORALZ generator [36] was used for the $\mu^+\mu^-\gamma(\gamma)$ and $\tau^+\tau^-\gamma(\gamma)$ topologies. These generators include initial and final-state radiation, which is particularly important for the analyses with photons in the final states. Low-multiplicity 4-fermion final states produced in 2-photon interactions were modelled by using VERMASEREN [37].

Finally, SM processes with only photons in the final state are an important background to the analysis of excited neutral leptons with photonic decays. The RADCOR [38] program was used to simulate the process $e^+e^- \to \gamma\gamma(\gamma)$ and KORALZ was used to simulate the process $e^+e^- \to \nu\overline{\nu}\gamma(\gamma)$.

All signal and background MC samples were processed through the full OPAL detector simulation [39] and passed through the same analysis chain as the data.

3 Selection

The searches presented in this paper involve many different experimental topologies. Three classes of different analyses are used which rely on slightly different criteria for such details as track and cluster quality requirements and lepton identification methods. The first class of analyses includes the selections for high-multiplicity topologies, with hadronic jets in the final state from the hadronic CC decays of heavy leptons and the hadronic CC and NC decays of excited neutral and charged leptons. The second class includes selections for low-multiplicity topologies, and covers the photonic decays of excited charged leptons. The third class covers purely photonic event topologies arising from the photonic decays of excited neutral leptons.

3.1 High-Multiplicity Topologies

The searches for topologies with hadronic jets in the final state share a common high-multiplicity preselection. All charged tracks and calorimeter clusters are subjected to established quality criteria [11]. Events are required to have at least 8 tracks and 15 clusters. The total visible energy measured in the detector, $E_{\rm vis}$, calculated from tracks and clusters [41], must be greater than 20 GeV.

Global event properties after this preselection are shown in Figure 1, which compares data and MC distributions. The visible energy is well described for $E_{\rm vis} > 75$ GeV, where 2-fermion and 4-fermion processes dominate. For $E_{\rm vis} < 20$ GeV, the data are not as well modelled. This region is dominated by events from 2-photon processes, which are not a significant background to the majority of analyses described in this paper. After a cut of $E_{\rm vis} > 75$ GeV, the global event properties shown in Figure 1 (b-f) compare well between data and the SM expectation.

Figure 2 shows the energy distribution of identified electrons, muons, taus, and photons after the preselection. The lepton identification is similar to that described in [11], with modified

isolation requirements for the high-multiplicity selections. Identified electrons and muons must have more than 1.5 GeV of visible energy, and taus more than 3 GeV. In addition, leptons have to be isolated within a cone of 15°. The typical lepton identification efficiencies are 85-90% for electrons and muons and 70% for taus.

3.1.1 Pair-Production of Heavy Leptons

L^+L^- Candidates give rise to final states produced from flavour-mixing decays into light leptons via $L \to \nu_e W$, $L \to \nu_\mu W$, and $L \to \nu_\tau W$. The resulting topologies, $\nu\nu WW$, consist of the decay products of the two W-bosons along with missing transverse momentum. The main background to this selection is SM W-pair production. To optimize the sensitivity, selections for all high-multiplicity final states $\nu\nu$jjjj, $\nu\nu e\nu$jj, and $\nu\nu\mu\nu$jj are performed, where "j" refers to a hadronic jet. The final state $\nu\nu\tau\nu$jj does not improve the sensitivity, and is not considered. In the selection for $\nu\nu$jjjj events, at least 12 GeV of missing momentum and at least 8 GeV of missing transverse momentum are required, and the missing momentum vector must not point along the beam direction ($|\cos(\theta_{\rm miss})| < 0.9$). In addition, the events must satisfy higher track (10) and cluster multiplicity (35) requirements, and are vetoed if a charged lepton is identified. The number of events after applying these selections is shown in Table 1 for data and for the SM expectation. The selection efficiency, including the W branching ratio, is about 17-25%, depending on the heavy lepton mass. In the selection of $\nu\nu e\nu$jj and $\nu\nu\mu\nu$jj events, an isolated lepton is required together with significant visible energy and missing transverse momentum. In this case, the selection efficiency, including the W branching ratio, is about 9-11%.

$N\bar{N}$ Candidates give rise to final states produced through the flavour-mixing decay into a light charged lepton, via $N \to eW$, $N \to \mu W$, or $N \to \tau W$. The topologies are defined as $\ell\ell WW$, where at least one W-boson decays hadronically and produces jets in the final state. At least two charged leptons of the same flavour are required and the jet resolution parameters have to be consistent with at least a 5-jet topology (isolated leptons are treated as "jets"). In order to optimize the sensitivity for the case $N \to \tau W$, the selection has been divided into $\tau\tau$jjjj topologies with fully-hadronic W-decays (2 charged leptons) and $\tau\tau\ell\nu$jj topologies with semileptonic W-decays, (3 charged leptons). The number of events after applying these selections is shown in Table 1. The signal efficiencies for a Dirac or Majorana lepton are about 50% for $N \to eW$, 57% for $N \to \mu W$, and 30-42% for $N \to \tau W$.

3.1.2 Pair-Production of Long-Lived Heavy Neutral Leptons

$N_L\bar{N}_L WW$ Candidates originate from the process $e^+e^- \to L^+L^-$ with $L^- \to N_L W^-$, where N_L is a stable or long-lived neutral heavy lepton which decays outside the detector. This production is possible if N_L is a member of a fourth-generation SU(2) doublet which does not mix with the three known lepton generations and satisfies $M_{L^\pm} > M_{N_L}$. This signal leads to very low visible energy if the mass difference, $\Delta M \equiv M_{L^\pm} - M_{N_L}$, is small. Events are required to have a visible energy between 8 and 90 GeV, the missing momentum vector must be at least 20% of the visible energy and lie within the barrel region, a minimum transverse energy of 12 GeV is required, and the topology should correspond to a pair of acoplanar jets ($> 14°$). The

	Mode	Topology	Data	Total Bkd
CC decays	LL $\to \nu\nu$WW	$\nu\nu$WW $\to \nu\nu$jjjj	67	74.0
	$\ell^*\ell^* \to \nu\nu$WW	$\nu\nu$WW $\to \nu\nu\nu$ejj	139	137.4
		$\nu\nu$WW $\to \nu\nu\nu\mu$jj	111	108.1
	NN $\to \ell\ell$WW	NN, $\nu^*\nu^* \to$ eeWW	2	1.3
	$\nu^*\nu^* \to \ell\ell$WW	NN, $\nu^*\nu^* \to \mu\mu$WW	3	2.4
		NN, $\nu^*\nu^* \to \tau\tau$jjjj	22	18.0
		NN, $\nu^*\nu^* \to \tau\tau\nu\ell$jj	2	1.2
	LL $\to$ $N_L N_L$WW	$N_L N_L$WW $\to$ $N_L N_L$jjjj	78	52.7
γ decays	$\ell^*\ell^* \to \ell\ell\gamma\gamma$	$e^*e^* \to ee\gamma\gamma$	2	3.3
		$\mu^*\mu^* \to \mu\mu\gamma\gamma$	1	1.1
		$\tau^*\tau^* \to \tau\tau\gamma\gamma$	0	0.9
	$\nu^*\nu^* \to \nu\nu\gamma\gamma$	$\nu^*\nu^* \to \nu\nu\gamma\gamma$	8	7.4

Table 1: Observed number of events in the data sample at $\sqrt{s}$ = 183 GeV and expected number of events from the background sources in the searches for the pair-production of heavy and excited leptons, where N_L is a stable or long-lived neutral heavy lepton which decays outside the detector.

total number of candidates and expected background are shown in Table 1. The typical signal efficiencies are about 30-40% for $\Delta M > 10$ GeV, dropping to a few per-cent for $\Delta M = 5$ GeV. A total of 78 events is observed, compared to an expected background of 52.7 events. The discrepancy may be due to mismodelling of the background, which is dominated by 2-photon processes with an estimated systematic error on the background of 20%. These events typically have energy deposited in the forward region ($|\cos(\theta)| > 0.9$), while from the signal MC one does not expect significant forward energy.

3.1.3 Pair-Production of Excited Leptons with hadronic decays

Excited leptons, which could be pair-produced at LEP2, are expected to decay dominantly via CC or photonic interactions, depending on their coupling assignments. The final states with both de-excitations via CC decays, $\ell^* \to \nu$W and $\nu^* \to \ell$W, are similar to the decay topologies of heavy leptons, L $\to \nu$W and N $\to \ell$W, so the same selections are applied, with the results shown in Table 1. The doubly-photonic decays give low-multiplicity topologies, and are discussed in Section 3.2.

3.1.4 Single-Production of Excited Leptons with hadronic decays

Candidates for the processes $\boldsymbol{\ell^{\pm *}\ell^{\mp} \to \ell^{\pm}\ell^{\mp}}$Z and $\boldsymbol{\nu_\ell{}^*\nu_\ell \to \nu_\ell\nu_\ell}$Z followed by the hadronic decay of the Z-boson are selected by requiring two identified leptons of the same flavour and significant visible energy or significant missing transverse momentum (>25 GeV), respectively. In the latter case, events containing charged leptons are vetoed. Accepted events have to be consistent with an acoplanar 2-jet topology. For the charged lepton final states, a kinematic fit is performed requiring energy and momentum conservation, and the fit probability has to be consistent with a $\ell^+\ell^-$jj final state. For the $\tau\tau$jj final state, to reduce the background further, additional cuts on the jet resolution parameter y_{34}, on the missing momentum vector, and on

the ratio of fitted tau energy to visible tau energy (> 1.15) are applied. The results for excited leptons are shown in Table 2 for data and for the SM expectation.

The selection efficiencies for excited leptons depend on the mass, and in the case of excited electrons also depend strongly on the coupling assignments for f and f' (see Section 1.2). For the case $f = -f'$, the s-channel production of excited electrons is dominant, and the selection efficiency is typically 30-50%. For the case $f \neq -f'$, the t-channel production of excited electrons dominates, in which the scattered electron is preferentially scattered at low angles and is not detected. The selection efficiency for this case is typically 7-10%. For excited muons and taus only s-channel production is allowed and the selection efficiencies range from 40-50% and 3-25%, respectively. The selection efficiencies for excited neutrinos are typically 30-40%.

To improve the sensitivity in the excited electron search for the case $f \neq -f'$ a dedicated selection for the e(e)jj channel has been designed, where the scattered electron is not observed in the detector. Events of this topology are selected by requiring exactly one electron to be identified. Tighter isolation cuts on the electron are applied and the event must have small missing transverse momentum (< 25 GeV), in order to reject eνjj final states from W-pair production. The event has to be consistent with a 3-jet topology, and events with high energy photons (> 50 GeV) in the final state are rejected to reduce background from radiative returns to the Z. The fitted kinematics must be consistent with having an undetected electron in the beam direction opposite to the detected electron. The selection efficiency for the case $f \neq -f'$ is typically 20-40% and the numbers of observed and expected events are shown in Table 2.

Candidates for the processes $\boldsymbol{\ell^{\pm}\ell^{\mp *} \rightarrow \ell^{\pm}\,\nu_{\ell}\mathrm{W}^{\mp}}$ and $\boldsymbol{\nu_{\ell}\nu_{\ell}^{*} \rightarrow \ell^{\pm}\,\nu_{\ell}\mathrm{W}^{\mp}}$ followed by a hadronic decay of the W boson are selected by requiring an isolated lepton to be identified. The total energy of the event must be at least 30% of the centre-of-mass energy. For the case $\ell = e$ and μ, the sum of the lepton energy and the missing transverse momentum must be at least 40% of the beam energy. Background from W-pair production is reduced by applying a kinematic fit to the jj$\ell\nu$ system, requiring energy and momentum-conservation. If the resulting masses of the jet-jet and $\ell\nu$ systems are consistent with the W mass, the event is rejected. For the case $\ell = \tau$, it is assumed that the direction of the τ is given by the direction of the leading particle of the τ candidate. Further background suppression is obtained by requiring that the ratio of energy to mass of the dijet system be greater than 1.1. The number of observed events and the SM expectation are shown in Table 2. The selection efficiency for these channels, for $f = -f'$, is typically from 20–30%.

For excited electron production in the case $f \neq -f'$, in which the scattered electron is not observed, a dedicated selection is applied. In this case, the total energy of the event must be at least 40% of the centre-of-mass energy, the missing transverse momentum must be at least 7.5% of the visible energy, and there must be no electron identified in the event. The event is forced into two jets, which are required to be acoplanar ($> 50^{\circ}$). The dijet mass M_{jj} must be consistent with the W mass (< 100 GeV) and the ratio of energy to mass of the dijet system must exceed 1.1. The number of observed events and the SM expectation are shown in Table 2. The selection efficiency for this channel, for $f \neq -f'$, ranges from 10–30%.

3.2 Low-Multiplicity Topologies

In this section the selection of photonic decays of singly-produced or pair-produced excited charged leptons is discussed. The final states consist of 2 like-flavour leptons and 1 or 2 photons. The lepton and photon identification and analysis techniques are described in Reference [11].

3.2.1 Pair-Production of Excited Leptons with photonic decays

Candidates for the process $\ell^*\ell^* \to \ell^+\,\ell^-\gamma\gamma$ are selected by requiring the identification of two leptons with the same flavour and of two photons. These particles must carry at least 80% of the centre-of-mass energy in the case of $e^+e^-\gamma\gamma$ and $\mu^+\mu^-\gamma\gamma$, and between 40% and 95% of the centre-of-mass energy in the case of $\tau^+\tau^-\gamma\gamma$. The background in the $\ell^+\ell^-\gamma\gamma$ topology from Bhabha scattering and di-lepton production is reduced by requiring the leptons and photons to be isolated, and the background from the doubly-radiative return process $e^+e^- \to Z\gamma\gamma \to \ell^+\ell^-\gamma\gamma$ is reduced by vetoing events with di-lepton masses close to the Z mass. The selection efficiencies are insensitive to the excited lepton mass and are about 54% for $e^{*+}e^{*-}$, 61% for $\mu^{*+}\mu^{*-}$, and 40% for $\tau^{*+}\tau^{*-}$. The number of observed events and the SM expectation is shown in Table 1.

3.2.2 Single-Production of Excited Leptons with photonic decays

Candidates for the process $\ell^*\ell \to \ell^+\ell^-\gamma$ are selected with a technique identical to the $\ell^+\ell^-\gamma\gamma$ selection, except that only one photon is required. Figure 3 shows the resulting $\ell^\pm\gamma$ invariant mass distributions.

To improve the efficiency for the excited electron search with $f \neq -f'$, giving rise to t-channel production, a dedicated search is performed for final states with a single electron and single photon visible in the detector, assuming the other electron is missing along the beam axis. Events with one electron and one photon carrying together at least 40% of the total centre-of-mass energy are selected. The photon is additionally required to have $|\cos(\theta_{\rm miss})| < 0.7$, greatly suppressing the Bhabha scattering background.

The number of observed events and the SM expectation are shown in Table 2, and the lepton-photon invariant masses for the selected events are shown in Figure 3. No peak is observed. The selection efficiencies are typically about 70% for e^*e and $\mu^*\mu$, and about 40% for $\tau^*\tau$. The excess in the $\tau^*\tau$ search is consistent with a statistical fluctuation in the SM $\tau^+\tau^-\gamma$ background.

3.3 Photonic final states

The search for singly- and pair-produced excited neutral leptons, $\nu^*\nu \to \nu\nu\gamma$ and $\nu^*\nu^* \to \nu\nu\gamma\gamma$, uses the OPAL search for photonic events with missing energy, described in [42]. The numbers

	Mode	Topology	Data	Total Bkd
NC decays	$\ell^*\ell \to \ell\ell$Z	$e^*e \to ee\,jj$	2	2.3
		$e^*e \to e(e)\,jj$	32	27.3
		$\mu^*\mu \to \mu\mu\,jj$	2	2.2
		$\tau^*\tau \to \tau\tau\,jj$	5	4.3
	$\nu^*\nu \to \nu\nu$Z	$\nu^*\nu \to \nu\nu\,jj$	23	22.9
CC decays	$\ell^*\ell \to \nu\ell$W	$e^*e \to \nu_e e\,jj$	13	18.4
		$e^*e \to \nu_e(e)\,jj$	18	17.6
		$\mu^*\mu \to \nu_\mu\mu jj$	6	6.7
		$\tau^*\tau \to \nu_\tau\tau jj$	23	27.7
	$\nu^*\nu \to \nu\ell$W	$\nu_e^*\nu_e \to \nu_e e\,jj$	13	18.4
		$\nu_\mu^*\nu_\mu \to \nu_\mu\mu jj$	6	6.7
		$\nu_\tau^*\nu_\tau \to \nu_\tau\tau jj$	23	27.7
γ decays	$\ell^*\ell \to \ell\ell\gamma$	$e^*e \to ee\,\gamma$	25	39.9
		$e^*e \to (e)e\,\gamma$	195	213.7
		$\mu^*\mu \to \mu\mu\,\gamma$	17	16.5
		$\tau^*\tau \to \tau\tau\,\gamma$	34	22.9
	$\nu^*\nu \to \nu\nu\gamma$	$\nu^*\nu \to \nu\nu\,\gamma$	4	3.5

Table 2: Observed number of events in the data sample at $\sqrt{s}$ = 183 GeV and expected number of events from the background sources for the searches for the single-production of excited leptons. The symbol (e) indicates topologies in which one scattered electron is not observed in the detector.

of selected events and expected backgrounds are listed in Tables 1 and 2 for pair- and single-production, respectively. For excited neutrinos in the mass range 70–180 GeV, the selection efficiencies are 70% and 10–70% for pair- and single-production, respectively.

4 Results

The numbers of expected signal events are evaluated from the production cross-sections, the integrated luminosity, and the estimated detection efficiencies of the various analyses.

The systematic errors on the number of expected signal and background events are estimated from: the statistical error of the MC estimates (1-10%), the error due to the interpolation used to infer the efficiency at arbitrary masses from a limited number of MC samples (2-15%), the error on the integrated luminosity (0.6%), the uncertainties in modelling the lepton identification cuts and in the photon conversion finder efficiency (2-8%), and the error due to uncertainties of the energy scale, energy resolution, and error parameterisations (1-4%). The errors are considered to be independent and are added in quadrature to give the total systematic error which is taken into account for the limit calculations.

In the case of pair-production searches, the production cross-section is relatively model-independent, and limits on the masses of the heavy or excited leptons can be obtained directly. For the flavour-mixing heavy lepton decays in which the pair-produced heavy leptons undergo CC decays into light leptons, 95% confidence level (CL) lower limits on the mass of the heavy lepton are shown in Table 3. The results are given for both Dirac and Majorana heavy neutral

Mode		Mass Limit (GeV)
$N \to eW$	Dirac	88.0
	Majorana	76.0
$N \to \mu W$	Dirac	88.1
	Majorana	76.0
$N \to \tau W$	Dirac	71.1
	Majorana	53.8
$L \to \nu_\ell W$		84.1

Table 3: 95% CL lower mass limits on unstable neutral and charged heavy leptons obtained from the data collected at $\sqrt{s} = 183$ GeV.

Flavour	Coupling	Dominant Decay	Mass Limit (GeV)
e^*	$f = f'$	Photonic	91.3
μ^*	$f = f'$	Photonic	91.3
τ^*	$f = f'$	Photonic	91.2
e^*	$f = -f'$	CC	86.0
μ^*	$f = -f'$	CC	86.0
τ^*	$f = -f'$	CC	86.0
e^*	Any f and f'		84.6
μ^*	Any f and f'		84.7
τ^*	Any f and f'		84.5

Table 4: 95% CL lower mass limits for the different charged excited leptons obtained from the pair production searches. The coupling assumption affects the dominant branching ratio.

leptons. These results are valid for a mixing angle squared, ζ^2, greater than about 10^{-12} radians^2. For the decays of charged heavy leptons into a massless neutral lepton, $L \to \nu_\ell W$, the searches for the $\nu\nu$jjjj decay and for the $\nu\nu$jj$\ell\nu_\ell$ have been combined. Masses smaller than 84.1 GeV are excluded at the 95% CL.

In the case that a heavy charged lepton $L^\pm$ decays into a stable heavy neutral lepton, N_L, the exclusion region depends on both M_L and M_{N_L}. In order to optimize the sensitivity of the analysis, a scan is performed in steps of ΔM. At each point, the expected minimum and maximum visible energy, (E_{min}, E_{max}), are calculated analytically, and the corresponding number of observed and expected events is determined. The resulting region in (M_L, M_N) excluded at the 95% CL is given in Figure 4, together with the mean expected limit.

The mass limits on excited leptons are somewhat better than for the heavy lepton case, primarily due to the nature of the vector couplings which lead to larger production cross-sections [5]. The mass limits inferred from the pair-production searches are shown in Table 4 for charged excited leptons and in Table 5 for neutral excited leptons. The first two sections of each table give the mass limits in which the dominant decay mode is assumed to be either via photons or W bosons.

Flavour	Coupling	Dominant Decay	Mass Limit (GeV)
ν_e^*	$f = f'$	CC	91.1
ν_μ^*	$f = f'$	CC	91.1
ν_τ^*	$f = f'$	CC	83.1
ν_e^*	$f = -f'$	Photonic	91.2
ν_μ^*	$f = -f'$	Photonic	91.2
ν_τ^*	$f = -f'$	Photonic	91.2
ν_e^*	Any f and f'		90.5
ν_μ^*	Any f and f'		90.5
ν_τ^*	Any f and f'		81.5

Table 5: 95% CL lower mass limits for the different neutral excited leptons obtained from the pair production searches. The coupling assumption affects the dominant branching ratio.

In the single-production searches, the production cross-section depends on parameters within the model, so limits on those parameters, as a function of the new particle masses, are inferred instead. From the single production searches, 95% CL limits have been calculated on $\sigma \times$ BR for $e^+e^- \to \ell^*\bar{\ell}$, $\ell^* \to \ell V$ for the different particle types, including photonic decay results from $\sqrt{s} = 161$ GeV and 172 GeV, where the branching ratio, "BR", depends on the relative values of f and f'.

In general, the mass limits have been evaluated using a sliding window technique [11], taking into account the expected mass resolution for the eνjj, $\mu\nu$jj, $\tau\nu$jj topologies (CC decays) and the eeγ, $\mu\mu\gamma$, $\tau\tau\gamma$ topologies (photonic decays), or by taking into account the kinematically allowed mass limits for the $\nu\nu\gamma$ topologies (photonic decays). For the eejj, $\mu\mu$jj, and $\tau\tau$jj topologies (NC decays), a likelihood fit method has been used for the limit calculation [43]. The resulting limits on $\sigma \times$ BR are shown for excited charged leptons in Figure 5 and for excited neutral leptons in Figure 6 for all generations decaying via photonic, neutral current, and charged current processes. The $\sigma \times$ BR limits do not depend on the coupling assignments except for excited electrons, where the selection efficiencies depend on the ratio of t-channel and s-channel contributions, and the results are shown for the example assignments $f = \pm f'$. The limits for the photonic decays are valid only for one of the two coupling assignments, $f = +f'$ for excited charged leptons and $f = -f'$ for excited neutral leptons.

From the single-production searches, limits on the ratio of the coupling to the compositeness scale, f/Λ, can be inferred. The results are shown in Figure 7 for two coupling assumptions[1]. Since the branching ratio of the excited lepton decays via the different vector bosons is not known, examples of coupling assignments, $f = \pm f'$, are used to calculate these branching ratios and then the photonic, NC and CC decay results are combined for the limits.

A new method is used to infer limits on the coupling strength f_0/Λ, independently of the relative values of f and f'. Here f_0 is a generalized coupling constant defined as $f_0 = \sqrt{\frac{1}{2}(f^2 + f'^2)}$. It is also useful to define the parameter $\tan\phi_f = f/f'$; the previous coupling

[1] For the figures of coupling versus compositeness scale given in [11], an error was discovered in the cross-section formula used; the resulting limits on f/Λ were over-conservative for most values of the excited lepton mass. This error has been corrected in the present paper.

assignments then correspond to $\phi_f = \pi/4$ ($f = f'$) and $\phi_f = -\pi/4$ ($f = -f'$).

From the Lagrangian in Equation 1, the cross-section depends on f and f' in the following way:

$$\sigma \;= \frac{a_1\, f^2 \;+\; a_2\, f\, f' \;+\; a_3\, f'^2}{\Lambda^2} = \big(\frac{f_0}{\Lambda}\big)^2 \cdot A(\phi_f), \tag{2}$$

where $A(\phi_f) = 2 \cdot (a_1 \sin^2\phi_f + a_2 \sin\phi_f \cos\phi_f + a_3 \cos^2\phi_f)$. The coefficients a_1, a_2, and a_3 can be calculated from the matrix elements. The production cross-section and also the decay of the excited leptons depend on the coupling assumption and on the angle ϕ_f. The branching ratio is calculated using the formulae given in [5]. By combining both the production cross-section and the branching ratio, the likelihood function $L(N_s)$, which is a function of the number of observed signal events N_s, can be translated into a likelihood function depending on the coupling strength $\frac{f_0}{\Lambda}$:

$$L\big(\frac{f_0^2}{\Lambda^2}\big) \;=\; L\big(\frac{N_s}{A(\phi_f) \cdot BR(\phi_f) \cdot \epsilon(\phi_f) \cdot \mathcal{L}}\big) \quad , \tag{3}$$

where $\epsilon(\phi_f)$ is the total selection efficiency and $\mathcal{L}$ the integrated luminosity.

In the case of μ^*, τ^*, ν_μ^*, and ν_τ^* production the efficiency is constant, while the case of the single production of excited e^* and ν_e^* is more complicated. Due to the different ϕ_f - dependent contributions of the t-channel and the s-channel diagrams, the selection efficiency also depends on ϕ_f. Using a MC technique to determine the selection efficiency for arbitrary ϕ_f would not be practical because a large number of MC events would have to be simulated for different excited lepton masses. It turns out, however, that the selection efficiency can be written as:

$$\epsilon(\phi_f) \;=\; \frac{\sigma_{sel}}{\sigma_{gen}} = \;\frac{e_1\, f^2 \;+\; e_2\, ff' \;+\; e_3\, f'^2}{a_1\, f^2 \;+\; a_2\, ff' \;+\; a_3\, f'^2} = \frac{N(\phi_f)}{A(\phi_f)}, \tag{4}$$

with $N(\phi_f) = 2 \cdot (e_1 \sin^2\phi_f \;+\; e_2 \sin\phi_f \cos\phi_f \;+\; e_3 \cos^2\phi_f)$. The coefficients e_i can be calculated by evaluating the selection efficiencies from three MC samples generated with different values of ϕ_f.

The selection efficiencies for the different decay topologies and the cross-section vary strongly with ϕ_f in the case of single e^* production. In order to avoid numerical errors, one of the generated MC points has been chosen for the coupling assumption $f = -f'$, where the large t-channel contribution vanishes and the cross-section is smallest. After having calculated the coefficients describing the selection efficiencies, the error of this method has been tested by comparing the calculated selection efficiency for a given value of ϕ_f with the selection efficiency determined from a MC sample generated with the same ϕ_f value. The error is found to be small compared to the statistical error of the MC samples.

Finally, the results from different decay channels are combined:

$$L_{\ell^*}\big(\frac{f_0^2}{\Lambda^2}\big) = L_{\ell^* \to \ell\gamma}\big(\frac{f_0^2}{\Lambda^2}\big) \otimes L_{\ell^* \to \ell \mathrm{Z}}\big(\frac{f_0^2}{\Lambda^2}\big) \otimes L_{\ell^* \to \nu_\ell \mathrm{W}}\big(\frac{f_0^2}{\Lambda^2}\big) \quad . \tag{5}$$

The resulting likelihood functions from different decay topologies are combined and upper limits on $\frac{f_0^2}{\Lambda^2}$ are inferred as a function of the excited lepton mass by using the most conservative limit

as a function of ϕ_f. The limit on $\frac{f_0^2}{\Lambda^2}$ for any value of ϕ_f is determined and shown in Figure 8. Using a similar technique, from the searches for the pair-production of excited leptons, the mass limits independent of the values of f and f' are given in the last section of Tables 4 and 5 for charged and neutral excited leptons, respectively. Together these represent the first limits on the compositeness scale f_0/Λ which do not depend on the relative values of f and f'.

5 Conclusion

We have searched for the production of unstable heavy and excited leptons in a data sample corresponding to an integrated luminosity of 58 pb^{-1} at a centre-of-mass energy of 181-184 GeV, collected with the OPAL detector at LEP. No evidence for their existence was found. From the search for the pair-production of heavy and excited leptons, lower mass limits were determined. From the search for the single-production of excited leptons, upper limits on $\sigma \times \mathrm{BR}$ of $\mathrm{e^+e^-} \to \ell^*\bar{\ell}$, $\ell^* \to \ell V$ and upper limits on the ratio of the coupling to the compositeness scale were derived. These limits supersede the results in [11]. Limits on the masses of excited leptons and on the compositeness scale f_0/Λ are established independent of the relative values of the coupling constants f and f'.

Acknowledgements

We particularly wish to thank the SL Division for the efficient operation of the LEP accelerator at all energies and for their continuing close cooperation with our experimental group. We thank our colleagues from CEA, DAPNIA/SPP, CE-Saclay for their efforts over the years on the time-of-flight and trigger systems which we continue to use. In addition to the support staff at our own institutions we are pleased to acknowledge the
Department of Energy, USA,
National Science Foundation, USA,
Particle Physics and Astronomy Research Council, UK,
Natural Sciences and Engineering Research Council, Canada,
Israel Science Foundation, administered by the Israel Academy of Science and Humanities,
Minerva Gesellschaft,
Benoziyo Center for High Energy Physics,
Japanese Ministry of Education, Science and Culture (the Monbusho) and a grant under the Monbusho International Science Research Program,
Japanese Society for the Promotion of Science (JSPS),
German Israeli Bi-national Science Foundation (GIF),
Bundesministerium für Bildung, Wissenschaft, Forschung und Technologie, Germany,
National Research Council of Canada,
Research Corporation, USA,
Hungarian Foundation for Scientific Research, OTKA T-029328, T023793 and OTKA F-023259.

References

[1] S.L. Glashow, J. Iliopoulos, and L. Maiani, Phys. Rev. **D2** (1970) 1285;
S. Weinberg, Phys. Rev. Lett. **19** (1967) 1264;
A. Salam, *Elementary Particle Theory*, ed. N. Svartholm (Almquist and Wiksells, Stockholm, 1968), 367.

[2] "Review of Particle Physics" R.M. Barnett *et al.*, Phys. Rev. D54 (1996).

[3] A. Djouadi, D. Schaile, C. Verzegnassi, *et al.*, Report of the Working Group "Extended Gauge Models" in Proceedings of the Workshop "e^+e^- Collisions at 500 GeV: The Physics Potential", P. Zerwas, (ed.) Report DESY 92-123A+B.

[4] A. Djouadi, Z. Phys. C63 (1994) 317, and references therein.

[5] F. Boudjema, A. Djouadi, and J.L. Kneur, Z. Phys. C57 (1993) 425.

[6] ALEPH Collaboration, D. Decamp *et al.*, Phys. Lett. B236 (1990) 511;
OPAL Collaboration, M.Z. Akrawy *et al.*, Phys. Lett. B240 (1990) 250;
OPAL Collaboration, M.Z. Akrawy *et al.*, Phys. Lett. B247 (1990) 448;
L3 Collaboration, B. Adeva *et al.*, Phys. Lett. B251 (1990) 321;
DELPHI Collaboration, P. Abreu *et al.*, Phys. Lett. B274 (1992) 230.

[7] OPAL Collaboration, G. Alexander *et al.*, Phys. Lett. B385 (1996) 433.

[8] L3 Collaboration, M. Acciarri *et al.*, Phys. Lett. B377 (1996) 304;
ALEPH Collaboration, D. Buskulic *et al.*, Phys. Lett. B384 (1996) 439.

[9] OPAL Collaboration, K. Ackerstaff *et al.*, Phys. Lett. B393 (1997) 217.

[10] L3 Collaboration, M. Acciarri *et al.*, Phys. Lett. B412 (1997) 189.

[11] OPAL Collaboration, K. Ackerstaff *et al.*, Eur. Phys. J. C1 (1998) 45.

[12] OPAL Collaboration, K. Ackerstaff *et al.*, Phys. Lett. B433 (1998) 195-208.

[13] DELPHI Collaboration, P. Abreu *et al.*, Eur. Phys. J. C8 (1999) 41.

[14] OPAL Collaboration, M.Z. Akrawy *et al.*, Phys. Lett. B257 (1990) 531;
ALEPH Collaboration, R Barate *et al.*, Eur. Phys. J. C4 (1998) 571-590;
ALEPH Collaboration, D. Decamp *et al.*, Phys. Lett. B250 (1990) 172;
DELPHI Collaboration, P. Abreu *et al.*, Z. Phys. C53 (1992) 41;
L3 Collaboration, M. Acciarri *et al.*, Phys. Lett. B353 (1995) 136.

[15] OPAL Collaboration, G. Alexander *et al.*, Phys. Lett. B386 (1996) 463.

[16] L3 Collaboration, M. Acciarri *et al.*, Phys. Lett. B370 (1996) 211;
DELPHI Collaboration, P. Abreu *et al.*, Phys. Lett. B380 (1996) 480;
ALEPH Collaboration, D. Buskulic *et al.*,Phys. Lett. B385 (1996) 445.

[17] OPAL Collaboration, K. Ackerstaff *et al.*, Phys. Lett. B391 (1997) 197.

[18] DELPHI Collaboration, P. Abreu *et al.*, Phys. Lett. B393 (1997) 245;
L3 Collaboration, M. Acciarri *et al.*, Phys. Lett. B401 (1997) 139.

[19] L3 Collaboration, M. Acciarri *et al.*, CERN-EP/99-138, October 1999, accepted by Phys. Lett. B.

[20] H1 Collaboration, I. Abt *et al.*, Nucl. Phys. B396 (1993) 3;
ZEUS Collaboration, M. Derrick *et al.*, Z. Phys. C65 (1994) 627;
H1 Collaboration, S. Aid *et al.*, Nucl. Phys. B483 (1997) 44.

[21] OPAL Collaboration, G. Alexander *et al.*, Phys. Lett. B377 (1996) 222.

[22] OPAL Collaboration, K. Ackerstaff *et al.*, Phys. Lett. B391 (1997) 221;
OPAL Collaboration, K. Ackerstaff *et al.*, Eur. Phys. J. C2 (1998) 441

[23] OPAL Collaboration, K. Ahmet *et al.*, Nucl. Instr. Meth. A305 (1991) 275;
O. Biebel *et al.*, Nucl. Instr. Meth. A323 (1992) 169 ;
M. Hausschild *et al.*, Nucl. Instr. Meth. A314 (1992) 74;
B.E. Anderson *et al.*, IEEE Trans. Nucl. Sci. 41 (1994) 845;
S. Anderson *et al.*, Nucl. Instr. Meth. A403 (1998) 326.

[24] Super-Kamiokande Collaboration, Y. Fukuda *et al.*, Phys.Rev.Lett. 81 (1998) 1562-1567.

[25] MACRO Collaboration, M. Ambrosio *et al.*, hep-ex/9908066, 31 Aug 1999.

[26] M. Gell-Mann, P. Ramond, and R. Slansky, Rev. Mod. Phys. 50 (1978) 721;
T. Yanagida, Phys. Rev. D20 (1979) 2986.

[27] E. Nardi, E. Roulet, and D. Tommasini, Phys. Lett. B344 (1995) 225.

[28] R. Tafirout and G. Azuelos, "A Heavy Fermion and Excited Fermion Monte Carlo Generator for e^+e^- Physics", accepted by Comp. Phys. Comm.

[29] J.H. Kühn, A. Reiter, and P.M. Zerwas, Nucl. Phys. B272 (1986) 560.

[30] T. Sjöstrand, Comp. Phys. Comm. 82 (1994) 74.

[31] J. Fujimoto *et al.*, Comp. Phys. Comm. 100 (1996) 128.

[32] R. Engel and J. Ranft, Phys. Rev. D54 (1996) 4244.

[33] G. Marchesini *et al.*, Comp. Phys. Comm. 67 (1992) 465.

[34] S. Jadach, W. Placzek, and B.F.L. Ward, Phys. Lett. B390 (1997) 298.

[35] D. Karlen, Nucl. Phys. B289 (1987) 23.

[36] S. Jadach, B.F.L. Ward, and Z. Wąs, Comp. Phys. Comm. 79 (1994) 503.

[37] R. Bhattacharya, J. Smith, and G. Grammer, Phys. Rev. D15 (1977) 3267;
J. Smith, J.A.M. Vermaseren, and G. Grammer, Phys. Rev. D15 (1977) 3280.

[38] F.A. Berends and R. Kleiss, Nucl. Phys. B186 (1981) 22.

[39] J. Allison *et al.*, Nucl. Instr. Meth. A317 (1992) 47.

[40] N. Brown and W.J. Stirling, Phys. Lett. B252 (1990) 657;
S. Bethke, Z. Kunszt, D. Soper, and W.J. Stirling, Nucl. Phys. B370 (1992) 310;
S. Catani *et al.*, Nucl. Phys. B269 (1991) 432;
N. Brown and W. J. Stirling, Z. Phys. C53 (1992) 629.

[41] OPAL Collaboration, M.Z. Akrawy *el al.*, Phys. Lett. B253 (1990) 511.

[42] OPAL Collaboration, G. Abbiendi et al, Eur. Phys. J. C8 (1999) 23.

[43] L. Lyons, *Statistics for Nuclear and Particle Physicists*, Cambridge University Press, Cambridge (1986).

[44] OPAL Collaboration, G. Alexander *et al.*, Z. Phys. C52 (1991) 175.

[45] M. Hauschild *et al.*, Nucl. Instr. and Meth. A314 (1992) 74.

[46] OPAL Collaboration, R. Akers *et al.*, Phys. Lett. B327 (1994) 411.

[47] OPAL Collaboration, P. Acton *et al.*, Z. Phys. C58 (1993) 523.

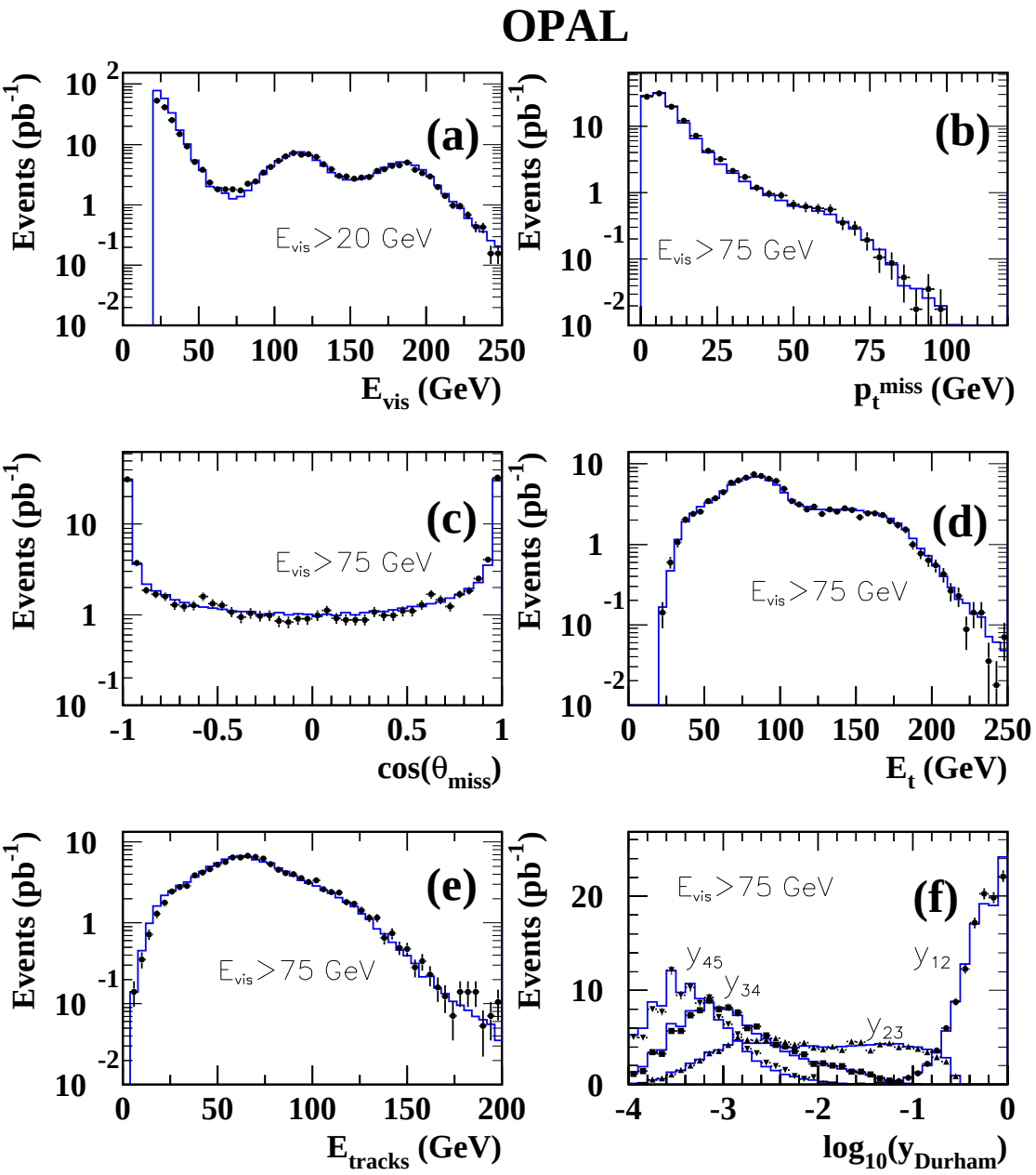

Figure 1: Global event properties after preselection cuts for the high-multiplicity selections. Figure (a) is the visible energy, (b) the missing transverse momentum, (c) the cosine of the polar angle of the missing momentum vector, (d) the transverse energy, (e) the summed energy measured from tracks, and (f) the logarithm of the jet resolution parameters y_{12}, y_{23}, y_{34}, and y_{45}, using the Durham jet-finding algorithm [40]. For figures (b-f) the two-photon background is reduced by requiring $E_{\rm vis} > 75$ GeV. In all figures, the filled symbols are the data and the solid line is the SM background prediction.

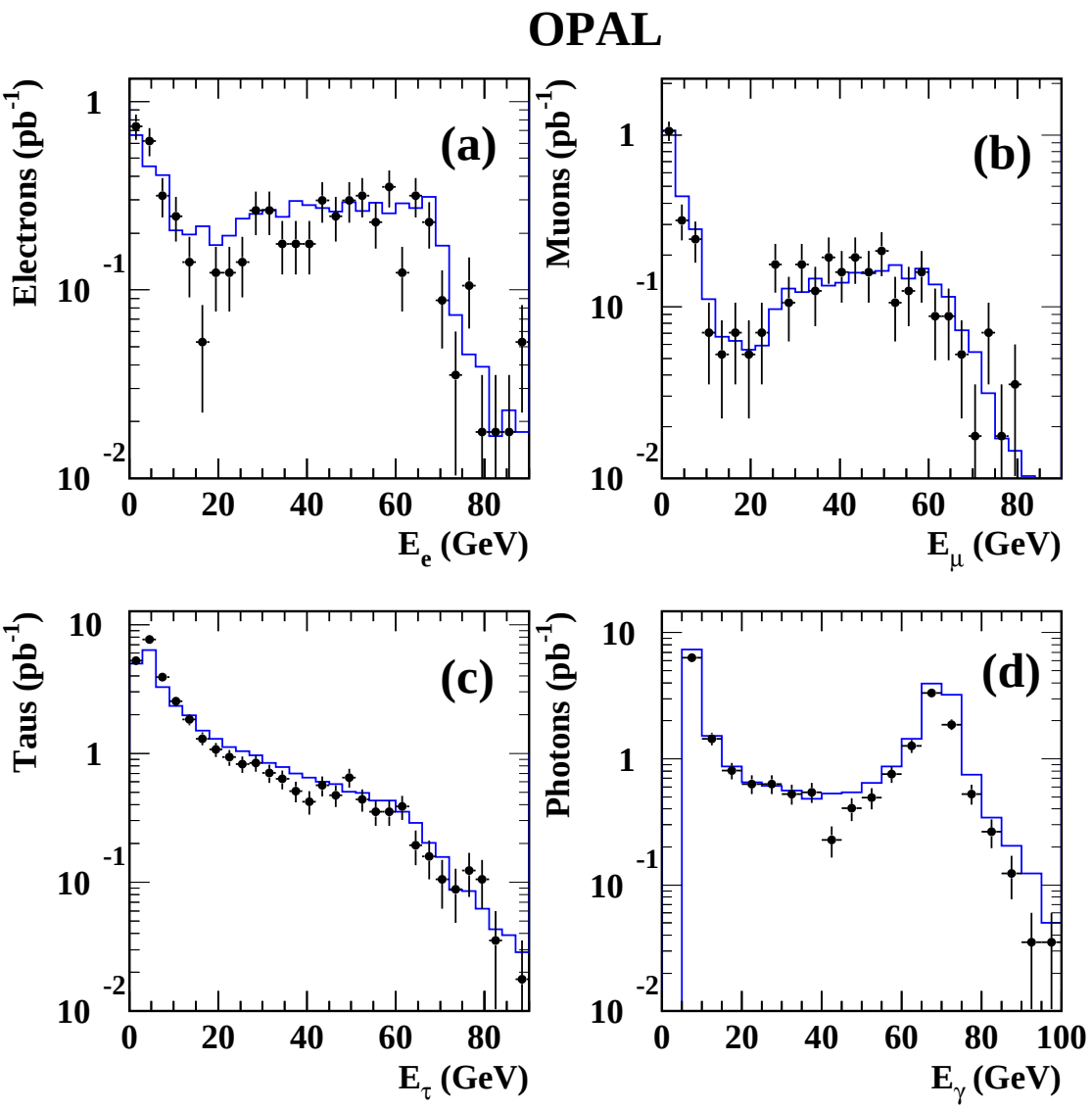

Figure 2: Particle identification after preselection cuts. The figures show the measured energy of (a) identified electrons, (b) identified muons, (c) identified taus, and (d) identified photons. In all figures, the filled circles are the data and the solid line is the sum of all SM background MC.

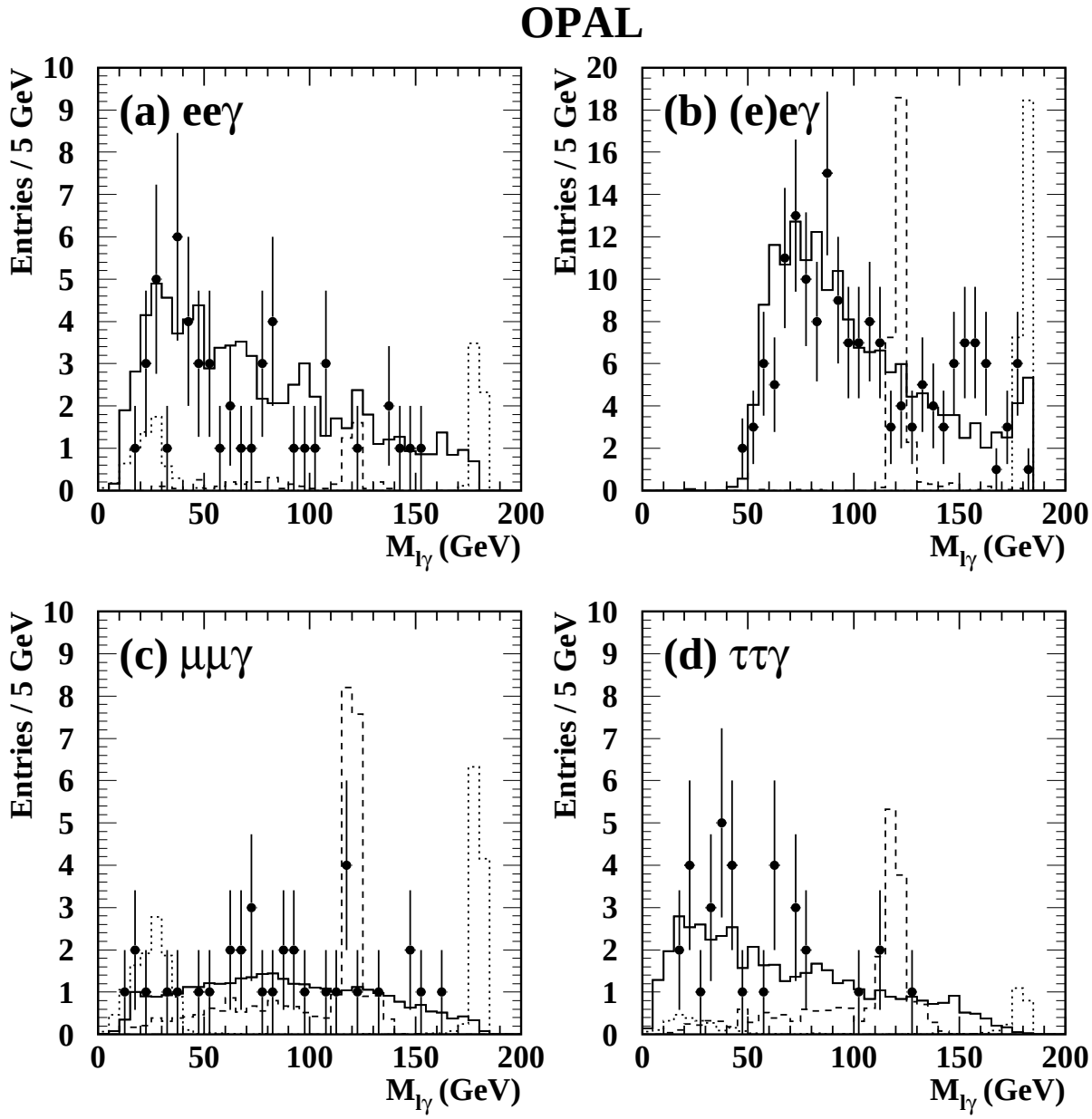

Figure 3: Lepton-photon invariant mass distributions for (a) $e^+e^-\gamma$, (b) (e)eγ, (c) $\mu^+\mu^-\gamma$ and (d) $\tau^+\tau^-\gamma$. The filled circles are the data, the solid line is the sum of all SM background MC, and the dashed and dotted lines show example signal MC with excited leptons masses of 120 and 180 GeV, respectively. There are two entries per event, due to the different mass combinations, resulting in a reflection peak at lower masses. The signal MC normalization is arbitrary.

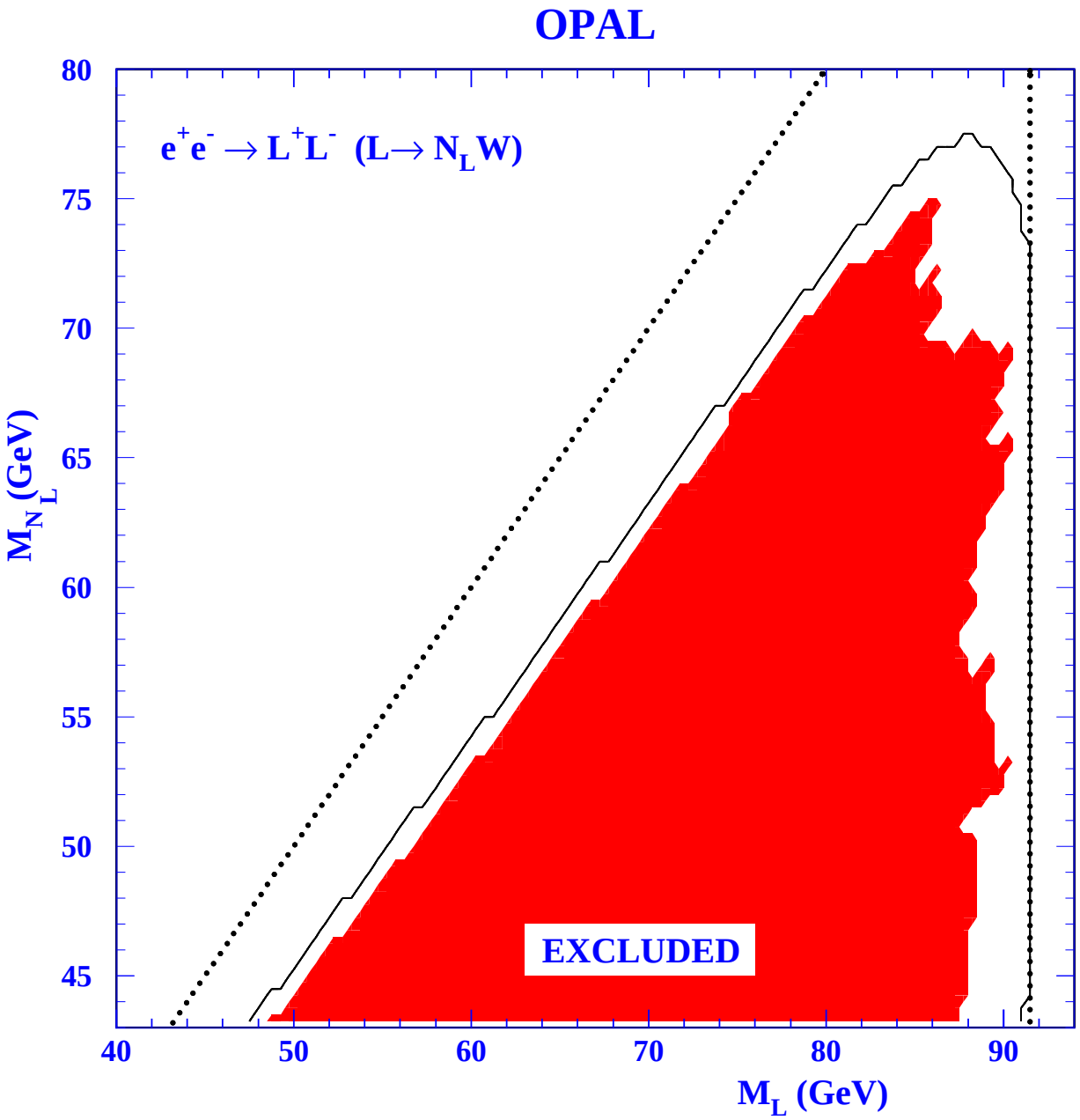

Figure 4: Excluded region in the $(M_{\mathrm{L}}, M_{\mathrm{N_L}})$ plane for L^+L^- production in the $\mathrm{L}^- \to \mathrm{N_L W}^-$ case, where $\mathrm{N_L}$ is a stable or long-lived neutral heavy lepton which decays outside the detector. The filled area represents the region excluded at the 95% CL. The dashed vertical line represents the kinematic limit, while the diagonal line corresponds to $\Delta M \equiv M_{\mathrm{L}} - M_{\mathrm{N_L}} = 0$.
The dark contour line shows the mean expected limit.

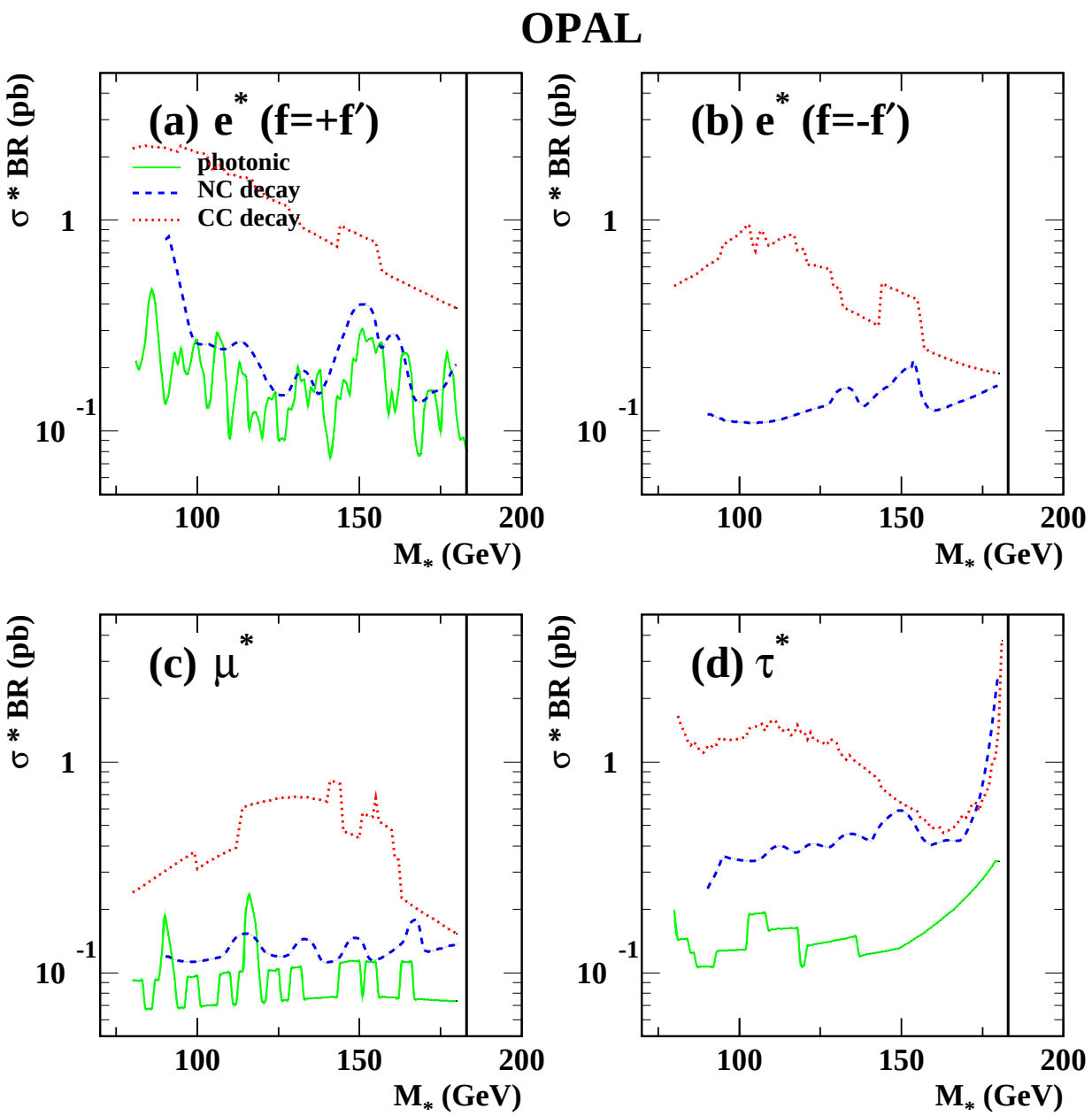

Figure 5: Upper limits at the 95% CL on the $\sigma \times BR$ of $e^+e^- \to \ell^*\bar{\ell}$, $\ell^* \to \ell V$ for the single-production of (a) e^* with $f = f'$, (b) e^* with $f = -f'$, (c) μ^*, and (d) τ^*. The photonic decay is represented by the full line, the NC decay by the dashed line, and the CC decay by the dotted line. For single μ^* and τ^* production the selection efficiency does not rely on the coupling assignment. For $f = -f'$ the photonic decay of e^* is forbidden. The symbol M_* represents the mass of the excited lepton.

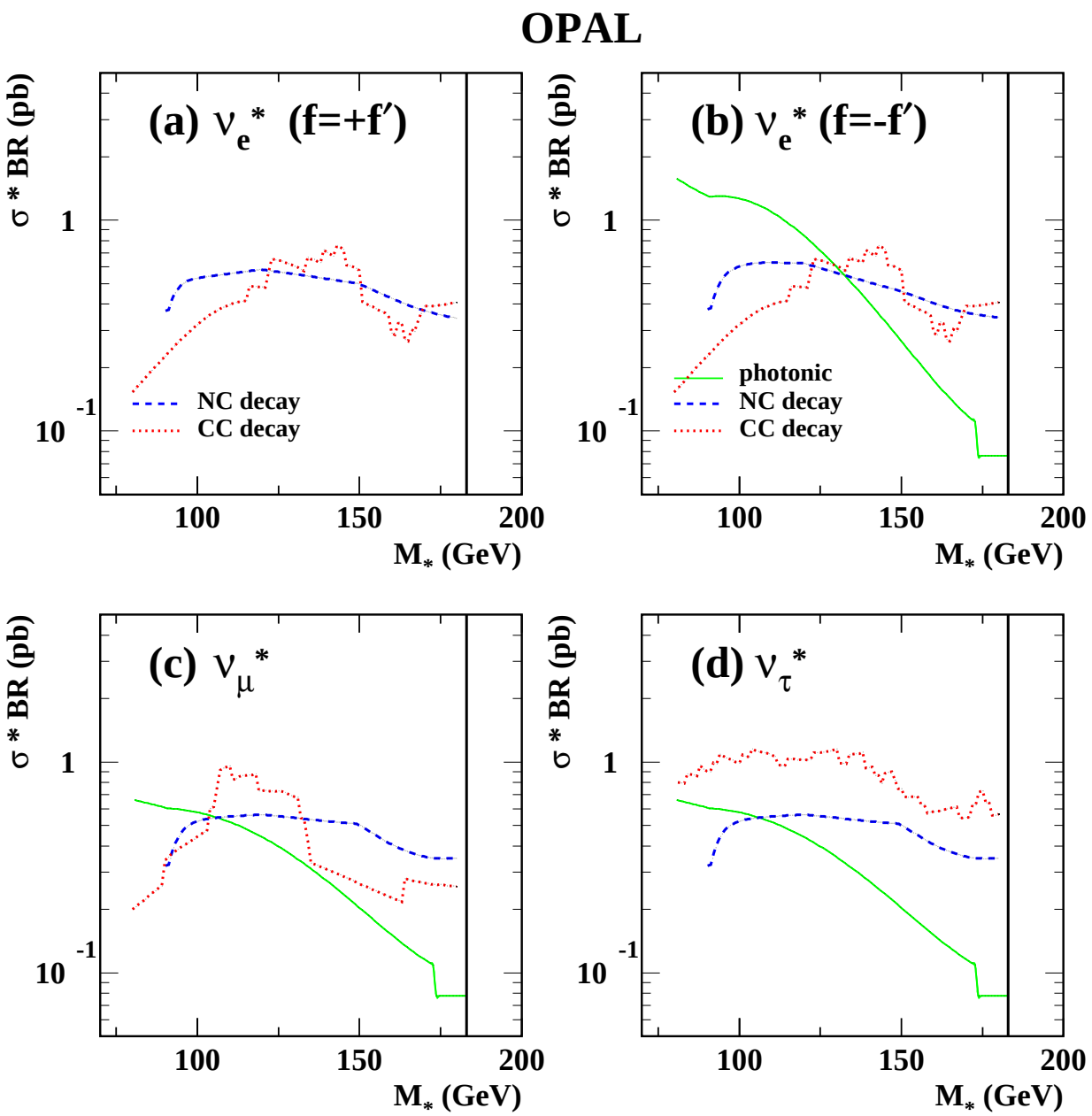

Figure 6: Upper limits at the 95% CL on the $\sigma \times BR$ of $e^+e^- \to \ell^*\bar{\ell}$, $\ell^* \to \ell V$ for the single-production of (a) ν_{e^*} with $f = f'$, (b) ν_{e^*} with $f = -f'$, (c) ν_μ^*, and (d) ν_τ^*. The photonic decay is represented by the full line, the NC decay by the dashed line, and the CC decay by the dotted line. For single ν_μ^* and ν_τ^* production the selection efficiency does not rely on the coupling assignment. For $f = f'$ the photonic decay of ν_e^* is forbidden. The symbol M_* represents the mass of the excited lepton.

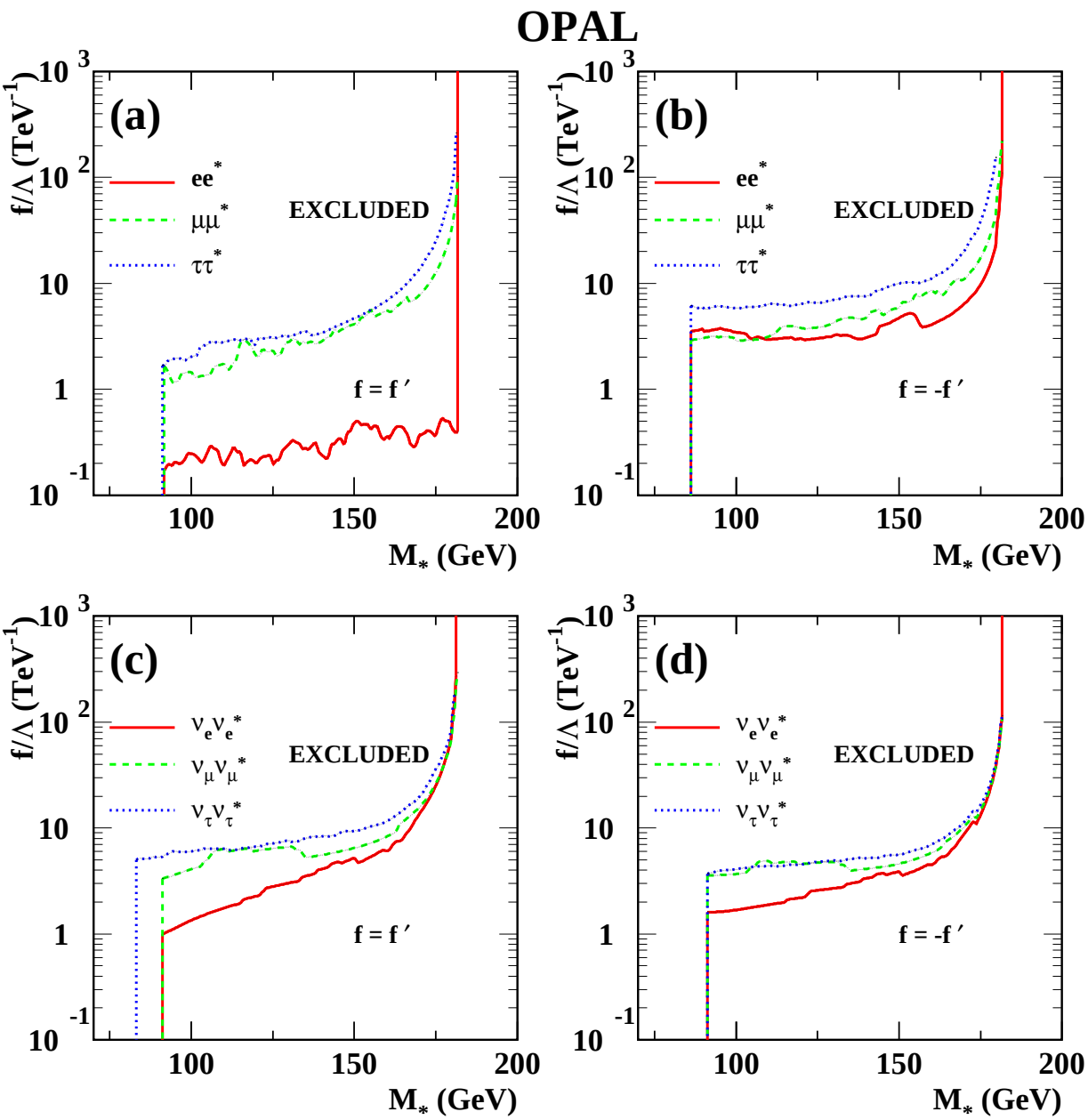

Figure 7: Upper limits at the 95% CL on the ratio f/Λ of the coupling strength to the compositeness scale, as a function of the excited lepton mass. (a) The limits on e*, μ^* and τ^* with $f = f'$; (b) the limits on e*, μ^* and τ^* with $f = -f'$, (c) the limits on ν_e^*, ν_μ^* and ν_τ^* with $f = f'$, and (d) the limits on ν_e^*, ν_μ^* and ν_τ^* with $f = -f'$. The regions above and to the left of the curves are excluded by the single- and pair-production searches, respectively. The symbol M_* represents the mass of the excited lepton.

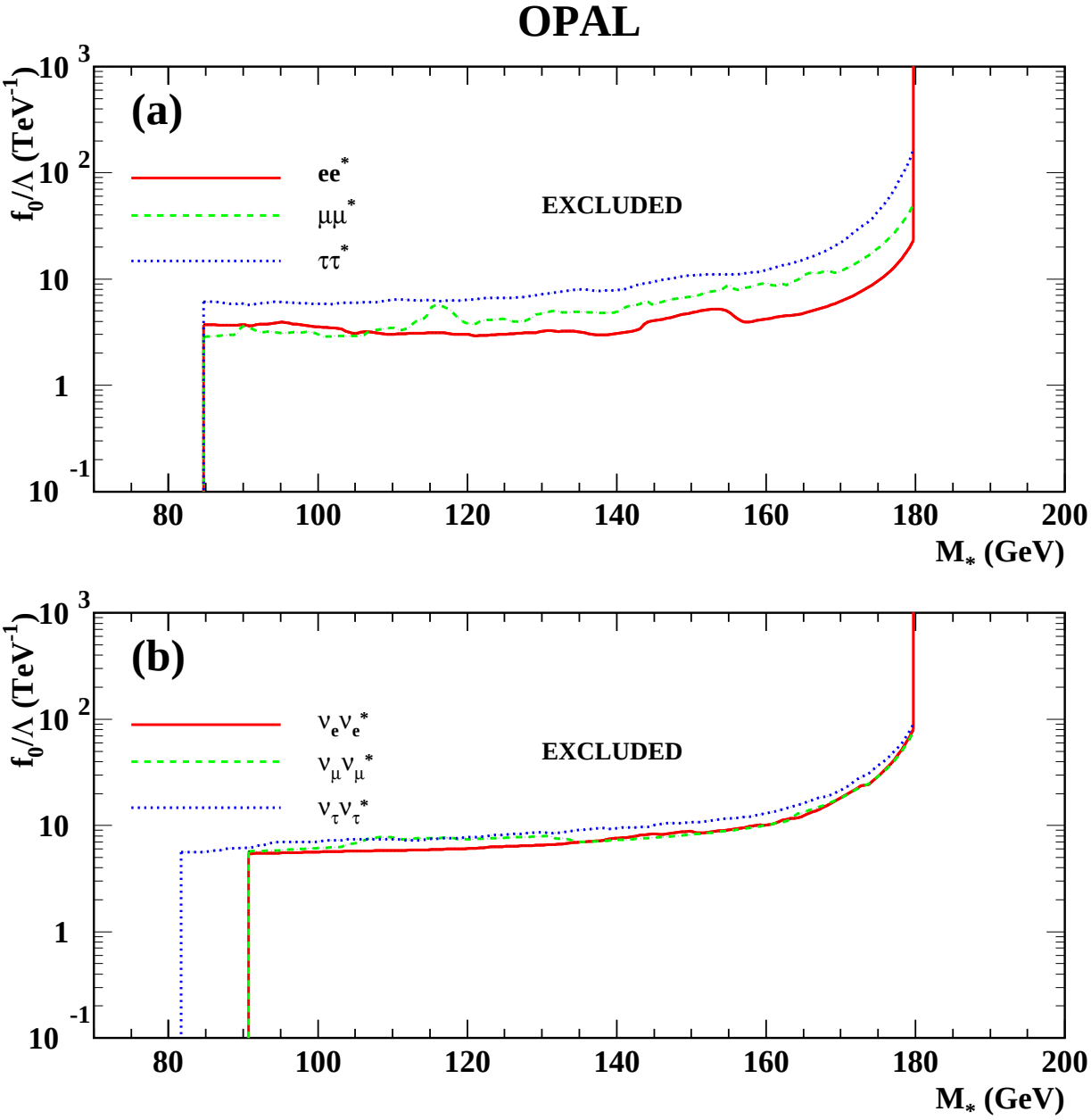

Figure 8: Upper limits at the 95% CL on the ratio f_0/Λ of the coupling strength to the compositeness scale, as a function of the excited lepton mass. (a) The limits on e*; μ^* and τ^* with arbitrary ϕ_f; (b) the limits on $\nu_e{}^*$, $\nu_\mu{}^*$ and $\nu_\tau{}^*$ with arbitrary ϕ_f. The regions above and to the left of the curves are excluded by the single- and pair-production searches, respectively. The symbol M_* represents the mass of the excited lepton.